



Short Communication

Numerical implementation of wavelet and fuzzy transform IFOC for three-phase induction motor



Sanjeevikumar Padmanaban ^{a,*}, Febin Daya J.L. ^b, Frede Blaabjerg ^c, Nazim Mir-Nasiri ^d, Ahmet H. Ertas ^e

^a Research and Development, Ohm Technologies, Chennai 600 122, India

^b School of Electrical & Electronics Engineering, Vellore Institute of Technology University, Chennai 600 127, India

^c Department of Energy Technology, Aalborg University, Pontoppidanstraede 101, 9220 Aalborg, Denmark

^d Department of Electrical and Electronics Engineering, Nazarbayev University, Astana 010000, Kazakhstan

^e Biomedical Engineering Department, Engineering Faculty, Karabuk University, Karabuk, Turkey

ARTICLE INFO

Article history:

Received 4 July 2015

Received in revised form

13 July 2015

Accepted 15 July 2015

Available online 14 August 2015

Keywords:

Speed compensator

Induction motor

AC drives

Indirect vector control

Wavelet transform

Fuzzy logic

Neural network

ABSTRACT

This article elaborates the numerical implementation of a novel, indirect field-oriented control (IFOC) for induction motor drive by wave-let discrete transform/fuzzy logic interface system unique combination. The feedback (speed) error signal is a mixed component of multiple low and high frequencies. Further, these signals are decomposed by the discrete wave-let transform (WT), then fuzzy logic (FL) generates the scaled gains for the proportional-integral (P-I) controller parameters. This unique combination improves the high precision speed control of induction motor during both transient as well as steady-state conditions. Numerical simulation model is implemented with proposed control scheme using Matlab/Simulink software and obtained results confirm the expectation.

© 2015, Karabuk University. Production and hosting by Elsevier B.V. This is an open access article under the CC BY-NC-ND license (<http://creativecommons.org/licenses/by-nc-nd/4.0/>).

1. Introduction

The speed control of three-phase induction motor (IM) is quite complex due to its nonlinear characteristics. Therefore, controlling the flux and torque parameters with proper decoupling is derived from speed reference feedback. Classical speed control (indirect/direct vector control) of IM drives uses proportional-integral (P-I) and/or proportional-integral-derivative (P-I-D) controllers that have constant gain values at all operating conditions. In addition, the slip calculation relies on rotor time constant, but it varies with operating conditions. These controllers are not adaptive in nature with respect to the operating condition. Neural network and fuzzy logic are said to be intelligent, used to overcome the above drawbacks [1–4]. But neural network controllers (NNC) do not involve analytical model of the complete system under test and do not have the ability to adapt it to change in control environment. Still, it is a tedious process to select appropriate neural controller architecture and its training neuron process. Moreover,

FL is the simplest of intelligent controller versions and uses expert knowledge to drive the system even if the system is undefined and also with parameter variation issues [5,6].

Wavelet transform (WT) used to perform multi-resolution analysis of the feedback signals extracts and detects the components of frequency signal at any interval, but represents in another form. Recent trends of intelligent wavelet controller are focused on the application of controlling ac electric drives [2–8]. However a systematic development and implementation of a wave-let fuzzy based speed compensator for IM control is yet to appear. This article focused on a novel, simple and straightforward wavelet-fuzzy integrated controller for the IFOC speed control of IM drive and investigated in numerical simulation software (Matlab/Simulink).

2. Discrete wavelet transformation algorithm

The WTs are the extended method of Fourier transforms where the multidimensional time-frequency domain representation is allowed. The popularity of the WTs is mainly due to their ability to concentrate the energy of the processed signal into finite number of coefficients. The mathematical expression of a signal can be given in WT as follows [5–7,9]:

* Corresponding author. Tel.: +91-98431-08228.

E-mail address: sanjeevi_12@yahoo.co.in (S. Padmanaban).

Peer review under responsibility of Karabuk University.

$$\omega t(\tau, s) = \frac{1}{s} \int x(t) \Psi^{*} \left(\frac{t-\tau}{s} \right) dt \quad (1)$$

where $s > 0$ depicts the window size, which determines resolution for the graded wavelet base $\psi(t - \tau/s)$ in time-frequency domains. The value of s parameter depends on frequency inversely. The discrete wavelet transform (DWT) of $x(t)$ signal can be written as:

$$WT_{m,n}x(t) = \int_{-\infty}^{\infty} x(t) \Psi_{m,n}^{*}(t) dt \quad (2)$$

where $\Psi^{*}(t)$ is the wave-let function representation and m, n are the dilation representation, the translational parameter. Discrete wavelet transform (DWT) is realized through cascaded stages of low- and high-pass-filter, followed by down sampling, which performs frequency dilation. The coefficients a^1 and d^1 constitute the first level of decomposition and can be mathematically represented as:

$$a^1[n] = \sum_{k=0}^{N-1} g[k]x[n-k] \quad (3)$$

$$d^1[n] = \sum_{k=0}^{N-1} h[k]x[n-k] \quad (4)$$

The second level approximation and detailed coefficient of length $N/2$ is expressed as below:

$$a^2[n] = \sum_{k=0}^{N/2-1} g[k]a^1[2n-k] \quad (5)$$

$$d^2[n] = \sum_{k=0}^{N/2-1} h[k]a^1[2n-k] \quad (6)$$

The filtering and down sampling process is continued until the desired level is reached.

Several methods are proposed in the literature, but the minimal description length (MDL) data criterion is the best suited selection of the optimum wave-let function. The MDL criterion can be defined as [7,9]:

$$DL(k, n) = \min \left\{ \begin{array}{l} \frac{3}{2} k \log N \\ + \frac{N}{2} \log \|\tilde{\alpha}_n - \alpha_n^{(k)}\|^2 \end{array} \right\} \quad (7)$$

$$0 \leq k < N; \quad 1 \leq n \leq M$$

Here k and n are the indices. Integer N states the length of the signal while M expresses the wave-let filters. The $\tilde{\alpha}_n$ is the wave-let

vector, obtained by the coefficients of the signal which is transformed by the wavelet filter. Where $\alpha^{(k)}_n = \Theta^k \tilde{\alpha}_n$ actually is a vector with k (non-zero) elements, Θ^k is the threshold value which keeps k largest element number in $\tilde{\alpha}_n$ and keeping all elements to null. For the number of coefficients k , the MDL criterion giving the minimum value is considered as the optimum one. The level of decomposition depends on the signal as well as the wave-let used for decomposition. The Shannon entropy criterion is best suited to find the decomposition at optimum level of the speed error-signal for motor drive applications. For the entropy of a signal $x(n) = \{x_1, x_2, x_3, \dots, x_N\}$, length N can be represented as [5]:

$$H(x) = - \sum_{n=0}^{N-1} |x(n)|^2 \log |x(n)|^2 \quad (8)$$

According to the Shannon entropy based criterion, the entropy of the signal in the next level (p) is higher than the previous ($p - 1$), that is, if as below:

$$H(x)_p \geq H(x)_{p-1} \quad (9)$$

then decomposition of signals can be stopped at level ($p - 1$) and ($p - 1$) represents the optimum level decomposition. The output of a P-I-D controller is given by:

$$u = k_p e + k_i \int e dt + k_d \frac{de}{dt} \quad (10)$$

In frequency domain, the proportional k_p parameter corresponds to the low frequency component, the integral k_i parameter corresponds to medium frequency component and the derivative k_d parameter corresponds to high-frequency component. The control signal for the compensator can be calculated from the approximate coefficients of DWT as [6–8]:

$$u_w = k_{d1} e_{d1} + k_{d2} e_{d2} + \dots + k_{dN} e_{dN} + k_{aN} e_{aN} \quad (11)$$

where $e_{d1}, e_{d2}, \dots, e_{dN}$ corresponds to the error-signal of the detail-components and e_{aN} is the approximate components of the error-signal. The gains $k_{d1}, k_{d2}, \dots, k_{dN}$ are used to tune the approximate components of the error-signal. Gain k_{aN} actually tunes the low frequency component of the error-signal [6,7,9]. The schematic of the wave-let fuzzy based speed compensator is shown in Fig. 1. The error in speed, which is the difference between the reference and actual speed, is applied as source to both the WT block and fuzzy logic control block. The WT decomposes the speed error into approximate and details components up to level two using DWT. The FLC operates on the error (speed) and the derivative of the error (speed)

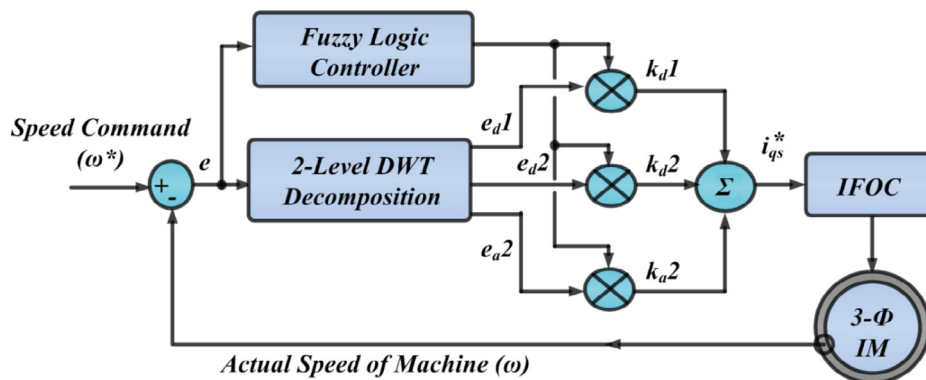


Fig. 1. Schematic of the proposed wavelet-fuzzy based speed compensator for IFOC IM drive.

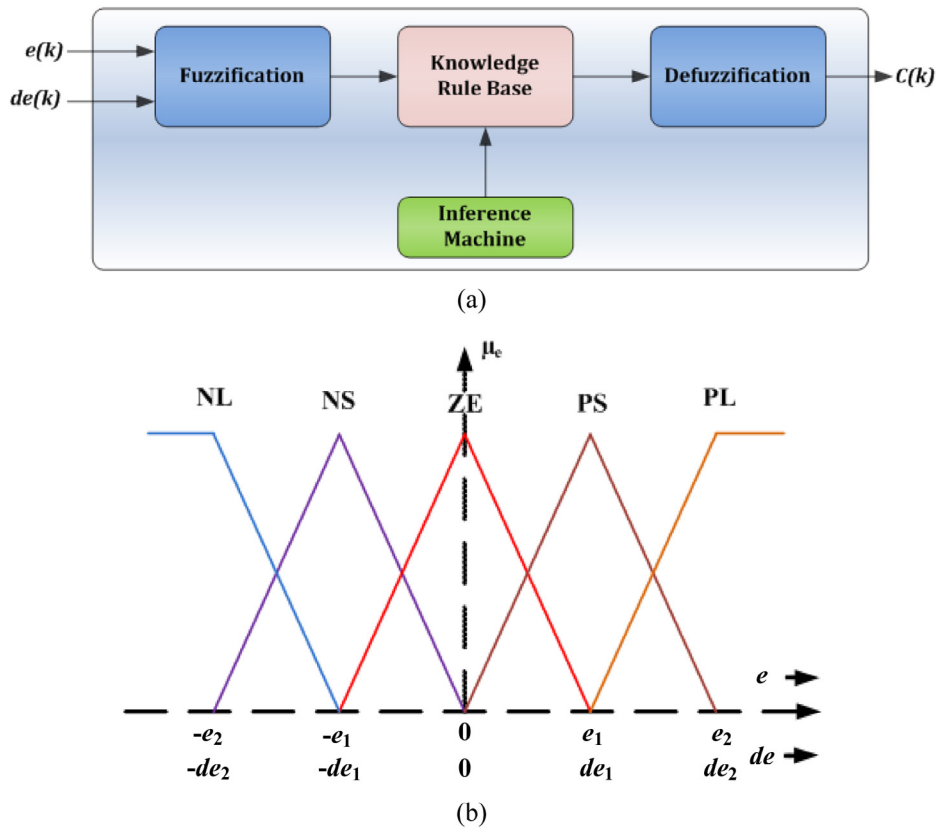


Fig. 2. (a) Fuzzy logic rule based system generalized structure. (b) Membership functions of the fuzzy logic controller for both, the error (e), and the change-in-error (de).

to produce the scaling gains k_{d1} , k_{d2} , and k_{a2} for the respective frequency components e_{d1} , e_{d2} and e_{a2} . The scaling gains are multiplied with their frequency components and summed up together to produce the control signal for the IFOC of IM drive.

Fig. 2a shows the schematic illustration of the FLC system and it consists of fuzzy interface, fuzzy rules, and de-fuzzification units. The two inputs to the FLC are the error (speed) and the change in error (difference between present speed-error and its immediate previous state), and the respective membership functions are given by Fig. 2b.

The first step in FLC begins with the membership (triangular) functions (Fig. 2b) which are converted from crisp-variables $e(k)$ and $de(k)$ to fuzzy-variables as $E(k)$ and $dE(k)$. Next, universe of discourse for each variable is divided further into five fuzzy sets: NL (negative-large), NS (negative-small), ZE (zero), PS (positive-small), and PL (positive-large). Each fuzzy-variable is a subset member with a degree of membership dwelling between zero (non-member) and one (full-member).

In the second step in FLC, the fuzzy-variables $E(k)$ and $dE(k)$ are processed by an inference engine with a set of controlled rules (5×5) matrix described in Table 1. Further, these rules are designed based on the dynamic of the error (speed) signal, which results in symmetrical matrix and is a generalized rule-based design with a 2-D phase plane. Hence, the rule is expressed in this form:

If 'x' is 'A' and 'y' is 'B' then 'z' is 'C'.

In this application max-min inference algorithms is used to space the fuzzy set values for the output fuzzy-variable $c(k)$. Therefore, the membership degree is equal to the maximum ($E \times dE$) membership degree, with x -product function. The outputs of the inference engine are converted to a crisp value in the de-fuzzification stage. It is to be noted in this work that the centroid algorithm is used

for de-fuzzification process, where the crisp values are determined by the center of gravity of the membership function. The definition of the spread of each partition or conversely the width and symmetry of the membership functions is generally a compromise between dynamic and steady-state accuracy. Equally spaced partitions and consequently symmetrical triangles are reasonable choices and executed in this work. The input variables are fuzzified using five membership functions normalized between +1 and -1. The scaling gains generated by the FLC are combined with the corresponding wave-let coefficients to generate the electromagnetic torque component command for the IM drive. The torque component command generated by the wave-let fuzzy controller is used to perform the IFOC of IM drive.

3. Numerical simulation test verification and results

Complete numerical model of the proposed wavelet-fuzzy based indirect field oriented controller for induction motor drive is developed in Matlab/Simulink software based on parameters taken from Table 2. The speed response of the ac motor drive is tested under different working condition, in particular step increment/

Table 1
Matrix formulation (5×5) for fuzzy logic rules.

$e(k)$	$de(k)$				
	NL	NS	ZE	PS	PL
NL	NL	NL	NL	NS	ZE
NS	NL	NL	NS	ZE	PS
ZE	NL	NS	ZE	PS	PL
PS	NS	ZE	PS	PL	PL
PL	ZE	PS	PL	PL	PL

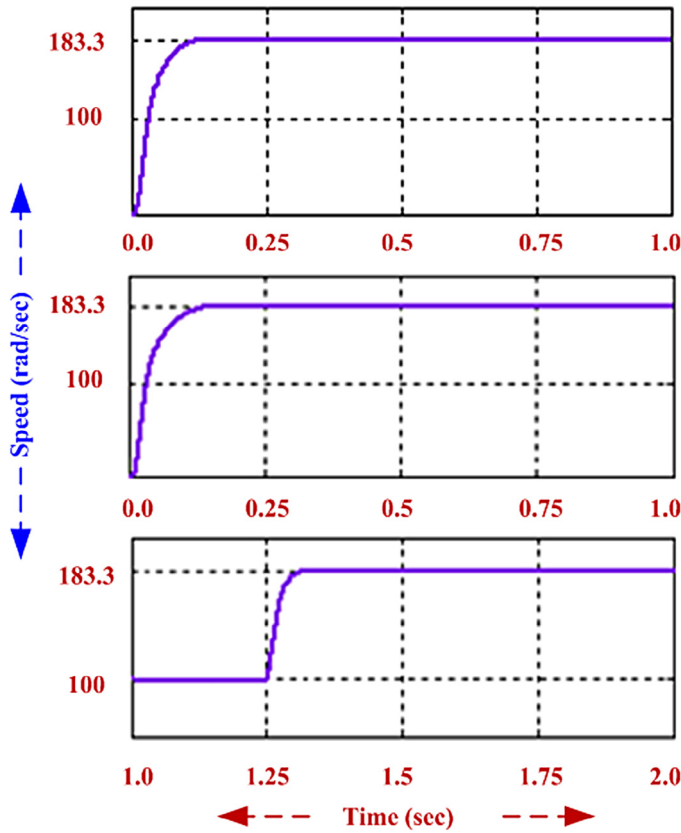


Fig. 3. Numerical simulation test, speed behavior of the induction motor controlled by the wavelet-fuzzy IFOC. Top: Starting at no-load with set speed command 183.3 rad/s; Middle: Starting at loaded condition of 2.5 Nm (set speed 183.3 rad/s); Bottom: No-load with step increase in set speed command 100 - 183.3 rad/s at t = 1.25 s.

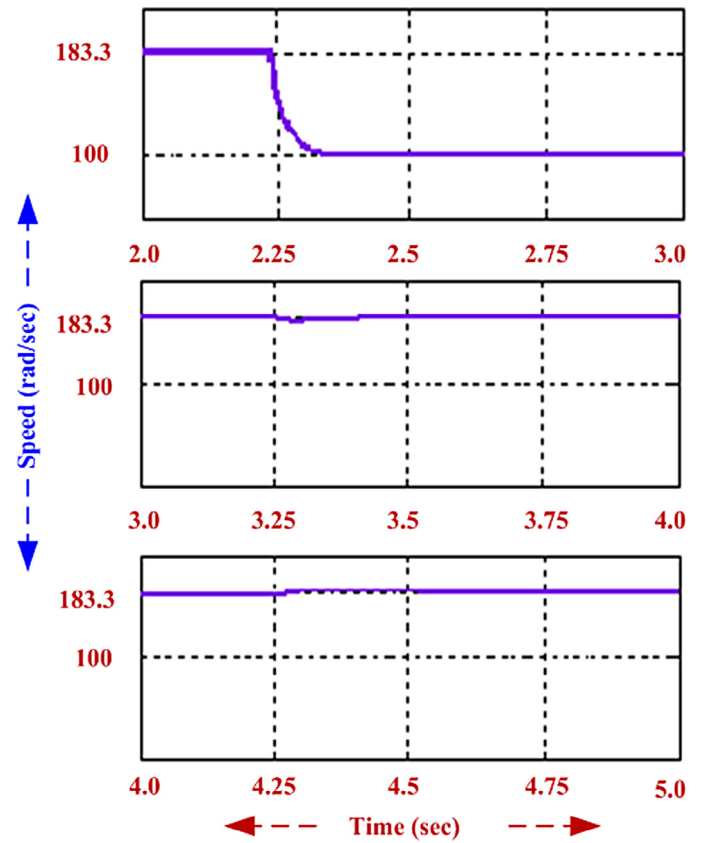


Fig. 4. Numerical simulation test, speed behavior of the induction motor controlled by the wavelet-fuzzy IFOC. Top: No-load with step decrease in set speed command 183.3 ~ 100 rad/s at t = 2.25 s; Middle: When 25% of rated load is applied at t = 3.25 s (set speed 183.3 rad/s); Bottom: When 25% of rated load is removed at t = 4.25 s (set speed 183.3 rad/s).

decrement of speed and load. Further, performance indices are tested to observe the rise time, peak over shoot, undershoot, steady-state error and root mean square error (RMSE) to prove the effectiveness of the proposed wavelet-fuzzy speed IFOC algorithm.

Fig. 3 and Fig. 4 show the complete speed behavior response of the induction motor controlled wavelet-fuzzy performances. In the first investigation, the transient speed response is illustrated in Fig. 3 (top), where the motor is started at no load with set speed command of 183.3 rad/s (i.e. the rated speed). In the second investigation, the speed behavior of the induction motor drive is tested, which is initially started with load of 2.5 Nm and a set speed command of 183.3 rad/s as shown in Fig. 3 (middle). In the third investigation, the speed behavior of the IM drive is tested for step increase in set speed command speed incremented in step from 100 rad/s to 183.3 rad/s at no load as shown in Fig. 3 (bottom). The speed is increased from 100 rad/s to 183.3 rad/s at t = 1.0 s. Step decremented in set speed command is tested from 183.3 rad/s to 100 rad/s as shown in Fig. 4 (top) at t = 2.25 s.

Table 2
Main parameters of AC motor drive.

Rated power	2	[hp]
Rated voltage	460	[V]
Rated frequency	60	[Hz]
Rated speed	1750	[rpm]
Number of pole pairs	2	
Stator resistance	2.12	[Ω]
Rotor resistance	2.08	[Ω]
Stator Inductance	5.97	[mH]

Further, speed behavior response tested under sudden loading of the induction motor is tested and shown in Fig. 4 (middle), where a load is applied at t = 3.25 s with the set speed command of 183.3 rad/s. Similarly, sudden removal of loading of the induction motor is tested and shown in Fig. 4 (bottom). For this case, the motor is started with the set speed command of 183.3 rad/s, a load of 25% of rated value is applied at t = 3.25 s and the load is removed at t = 4.25 s.

Finally, Table 3 gives the root mean square error (RMSE) values, which shows the good responses under different testing conditions by the values for both simulation and experimental investigation, further confirming the proposed wavelet-fuzzy controller suitability for the IFOC algorithm for industrial induction motor drive applications.

4. Conclusion

This article exploited a novel IFOC speed controller for a three-phase induction motor drive by the application of wavelet transform

Table 3
Observed performances indices of wavelet-fuzzy IFOC controller for IM drive.

Parameter speed	RMSE value
0–183.3 rad/s	26.32
100 rad/s – 183.3 rad/s	15.86
183.3 rad/s – 100 rad/s	19.21
180 rad/s, when load applied 2.5 Nm	31.29

with fuzzy interface system. Complete ac drive system along with the proposed control algorithm was numerically implemented in mathematical simulation software (Matlab/Simulink). Moreover, the dissimilated results in this paper confirm the robustness by its responses in terms of transient- and steady-state behavior. Finally, this numerical investigation concluded that the classical P-I controller can be replaced by the proposed compensator for (indirect/direct vector control) the high precision performances of industrial drives.

References

- [1] P. Vas, *Artificial-Intelligence-based Electrical Machines and Drives Application of Fuzzy, Neural, Fuzzy-neural, and Genetic-algorithm-based Techniques*, 1999. ISBN 978-0-19-859397-3.
- [2] M.A.S.K. Khan, M. Azizur Rahman, Implementation of a new wavelet controller for interior permanent-magnet motor drives, *IEEE Trans. Ind. Appl.* 44 (6) (2008) 1957–1965.
- [3] R.J. Wai, Development of new training algorithms for neuro-wavelet systems on the robust control of induction servo motor drive, *IEEE Trans. Ind. Electron.* 49 (6) (2002) 1323–1341.
- [4] M. Khan, M.A. Rahman, A novel neuro-wavelet-based self-tuned wavelet controller for IPM motor drives, *IEEE Trans. Ind. Electron.* 46 (3) (2010) 1194–1203.
- [5] J.L. Febin Daya, P. Sanjeevikumar, F. Blaabjerg, P.W. Wheeler, O. Ojo, Implementation of wavelet based robust differential control for electric vehicle application, *IEEE Trans. Power Electron.* (2015) doi:10.1109/TPEL.2015.2440297.
- [6] J.L. Febin Daya, V. Subbiah, P. Sanjeevikumar, Robust speed control of an induction motor drive using wavelet-fuzzy based self-tuning multi-resolution controller, *Int. J. Comput. Intell. Syst.* 6 (4) (2013) 724–738.
- [7] S. Parvez, Z. Gao, A wavelet based multiresolution PID controller, *IEEE Trans. Ind. Appl.* 41 (2) (2005) 537–543.
- [8] S.A. Saleh, M. Azizur Rahman, Analysis and real-time testing of a controlled single-phase wavelet-modulated inverter for capacitor-run induction motors, *IEEE Trans. Energy Convers.* 24 (1) (2009) 21–29.
- [9] G. Stang, T. Nguyen, *Wavelet and Wavelet Filter Banks*, Wellesley-Cambridge Press, Wellesley, 1997.